

Critical capture distances for highly charged ions above dielectric covered metal surfaces

R.E. Lake^{a,b,*}, J.M. Pomeroy^a, C.E. Sosolik^b

^a National Institute of Standards and Technology, Gaithersburg, Maryland 20899, USA

^b Department of Physics and Astronomy, Clemson University, Clemson, South Carolina 29634, USA

ARTICLE INFO

Article history:

Received 28 October 2010

Available online 7 December 2010

Keywords:

Highly charged ions
Ion-surface neutralization
Dielectric thin films

ABSTRACT

We model the first stage of the electronic interaction between an ion and a metal surface covered with a thin dielectric layer. Specifically, we seek to answer two questions. (i) As an ion approaches the surface from far away, does the first electron that it captures originate from the exposed dielectric layer or the metal underneath it? (ii) What is the ion's distance from the metal when the first electron is captured? To answer these questions, the classical potential that an electron is subject to during the interaction is calculated. The dielectric film is treated as a continuum with simple band structure. We input the parameters from recent experiments (Co with 1.5 nm thick Al₂O₃ film) and found that (i) the first capture proceeds from the metal, and (ii) the dielectric film extends the distance threshold for first capture compared to a metal with no film.

© 2010 Elsevier B.V. All rights reserved.

1. Introduction

When a slow highly charged ion (HCI) comes in close proximity with the reservoir of electrons in a solid state system, ion neutralization proceeds through a series of complex electronic relaxation processes. The well-known scenario for HCI neutralization is a multi-step process of electron capture and de-excitation that includes above-surface neutralization and formation of a “hollow atom” projectile [1]. The HCI's interaction with the solid begins as it approaches the surface, gaining kinetic energy due to its image attraction. When the ion has reached a critical distance R_c above the surface, it begins to capture its Q missing electrons into highly excited atomic states resulting in the formation of the neutral hollow atom. De-excitation of the electrons captured into excited states proceeds through Auger processes, re-ionization and screening of the excited electrons by electrons on the surface. Even for slow HCIs where the projectile velocity is less than the Bohr velocity ($v_p < v_{\text{bohr}}$), the timescale for electronic relaxation is long compared to the timescale for ion drift, and the HCI penetrates the solid while still in a highly excited state. Inner shell vacancies are then filled by electrons from the solid. These sub-surface electronic transitions lead to further Auger electrons as well as X-ray/photon emission.

The electron capture process during HCI neutralization at solid surfaces is well described for metal–vacuum interfaces by the clas-

sical over-the-barrier model (CBM) [2] and its application to insulator–vacuum interfaces [3]. As the HCI approaches, the critical distance for electron capture (R_c) can be approximated using classical potentials and the material's work function [4]. The electronic interaction between the HCI and surface takes place in a co-linear geometry, allowing for a one dimensional treatment of the potentials along the coordinate normal to the surface z . Therefore, for a metal target, an “active electron” crossing the vacuum barrier is subject to the potential:

$$V_{\text{CBM}}(z) = -\frac{Q}{|z-R|} + \frac{Q}{|z+R|} - \frac{1}{4z} \quad (1)$$

where the first term is the direct interaction between the electron and the ion (V_{int}), the second term is the interaction between the electron and ion's image charge (V_i) and the third term is the electron's self-image (V_{si}) attraction. Here the surface of the metal is set at $z=0$ and the ion is at a distance R outside its surface. Within CBM, the ion's first electron capture in the neutralization sequence occurs resonantly, over the vacuum barrier, when the ion reaches a position where its Coulomb potential reduces the vacuum energy barrier below the Fermi energy E_F and classical charge transfer is allowed. The potential in Eq. (1) predicts the ion's critical distance for above-surface electron capture analytically in terms of the work function W of the target material and the charge state Q of the projectile ion as $R_c \approx \sqrt{2Q}/W$ in atomic units. Contributions from tunneling through the thick barrier in the vacuum region are negligible.

In this article, we consider the HCI interaction with a solid state system composed of a bulk metal covered with a thin dielectric film. We modify the CBM by deriving the potential analogous to

* Corresponding author at: National Institute of Standards and Technology, Gaithersburg, Maryland 20899, USA. Tel.: +1 301 975 5862.

E-mail addresses: russell.lake@nist.gov, rlake@g.clemson.edu (R.E. Lake).

Eq. (1) for a metal target covered with a dielectric film, and examine the film's effect on R_c . The new critical distance for thin film covered metals is denoted as R'_c and found to be greater than R_c for parameters from recent experiments [5]. We also determine that the first electron capture (at R'_c) originates from the metal rather than the exposed insulating film. Atomic units (a.u.) are used throughout unless otherwise stated.

2. Model

To find the ion's distance from the metal surface at which the ion captures the first electron over-the-barrier R'_c , the potential $V(z)$ in the metal/insulator/vacuum was constructed. $V(z)$ is derived by modifying Eq. (1) to account for the effect of a thin dielectric film on the ion's interaction with the target. This potential is the sum of the interactions V_{int} , V_i and V_{si} depicted in Fig. 1. In the figure, the ion with charge Q is at a position R outside the metal, where the origin is set at the surface of the metal ($z = 0$). V_{int} is the attractive interaction between the electron and the ion. V_i is the repulsive interaction between the electron and the ion's image charge. V_{si} is the electron's self-image attraction. These are the same interactions expressed in Eq. (1), with the exception that the second and third terms are modified to account for the intermediary dielectric film on the surface of the metal, i.e., V_i and V_{si} are modified significantly by the presence of the thin film. These modifications were calculated using the dielectric continuum model (Ref.[6] and references therein) that treats the dielectric layer as a continuous film of thickness s and dielectric constant ϵ with a band gap E_g . The reference energy for electrons in the insulator is the conduction band minimum E_{cbm} instead of the vacuum energy. Additionally, modification of the potential to account for the dielectric film requires an infinite series of image charges to be positioned within the material. For example, the self-image V_{si} from Fig. 1 is defined piecewise as V_{in} inside the dielectric film and V_{out} in the vacuum,

$$V_{\text{in}} = E_{\text{cbm}} - \frac{e^2}{4\epsilon z} \quad 0 < z < s \quad (2)$$

$$V_{\text{out}} = -\frac{\beta e^2}{4(z-s)} + \frac{(1-\beta^2)e^2}{4\beta} \sum_{n=1}^{\infty} \frac{(-\beta)^n}{z-s+ns} \quad z > s, \quad (3)$$

where e is the charge of the electron and $\beta = (\epsilon - 1)/(\epsilon + 1)$. V_i is similarly modified by treating the ion's image potential with Eqs. (2) and (3) using the charge Q . The positions R_{im} and z_{im} of single image charges Q_{im} and e_{im} in Fig. 1 represent the "centroids" of

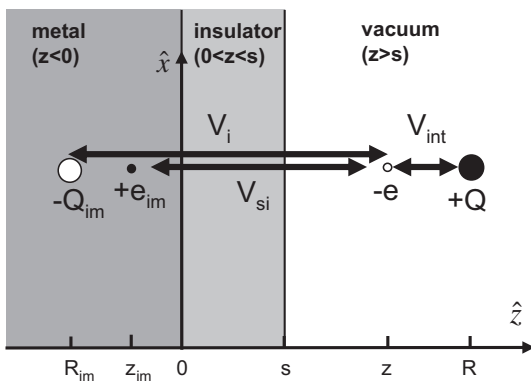


Fig. 1. Potential experienced by the "active electron" in the first stages of above-surface neutralization at a dielectric covered metal surface. V_{int} is the electron's interaction with the ion at position R , and V_i is the interaction with the ion's image charge at R_{im} . V_{si} is the electron's self-image. The dielectric film is parameterized by thickness s and dielectric constant ϵ . The origin ($z = 0$) is set at the surface of the metal.

the series of image charges expressed in Eqs. (2) and (3). A test charge in the dielectric region experiences attraction to its self-image in the metal (Eq. (2)). The image plane for this attraction is $z = 0$. Outside the dielectric in the vacuum region ($z > s$), there exists an image attraction toward the image plane at $z = s$ that is also determined by the thickness and permittivity of the layer [6] (Eq. (3)).

In Fig. 2, we plot the potential $V(z)$ for an electron in the solid constructed from the sum of the three interactions V_{int} , V_i and V_{si} shown schematically in Fig. 1. Here, V_i and V_{si} have been modified from Eq. (1) as shown in Eqs. (2) and (3) to account for the dielectric film. $V(z)$ is shown using parameters from recent experiments with a $Q = 44$ ion above an ultra-thin film target composed of a $s = 1.5$ nm thick Al_2O_3 film with permittivity $\epsilon = 9$ [5,7]. Dark gray represents filled electronic states, light gray represents unoccupied electronic states and white represents non-conducting regions in the vacuum and band gap of the insulator. Within the metal ($z < 0$ in Fig. 2) the work function $W = 5$ eV separates E_F from the vacuum level [7]. In the insulator film ($0 < z < s$), electrons exist in filled states of the valence band at or below E_{vbm} (in dark gray). The energy gap E_g separates the filled states in the insulator's valence band from the empty states in its conduction band. The band gap $E_g = 9.9$ eV of aluminum oxide [7] was used to define the position of valence band maximum E_{vbm} below E_{cbm} . E_{cbm} and E_{vbm} vary as the ion's potential perturbs the insulating bands, but E_g is held constant. E_F remains fixed throughout the interaction.

The energy difference between E_{cbm} and E_F is denoted as ϕ and was set at 1 eV as determined by tunneling spectroscopy measurements of $\text{Co}/\text{Al}_2\text{O}_3$ ($s = 1.5$ nm)/Co junctions [8]. The height of this barrier when $R \gg R'_c$ is set by the reference energy E_{cbm} in the dielectric film. Classical over-barrier transmission from electrons in the metal to the ion is limited by the potential barrier ϕ in the dielectric region $0 < z < s$ and W in the vacuum region $z > s$.

Far from the surface at $R = 1000$ a.u., interaction between the ion and electrons in the solid is negligible. Starting with the potential shown in Fig. 2, the ion is moved toward the surface (decreasing R) to find the position R'_c where the ion's potential pulls down the barrier and the first over-barrier transmission was allowed. As the ion moves toward the solid, the area of the (light gray) conducting region is increased and the (white) vacuum barrier

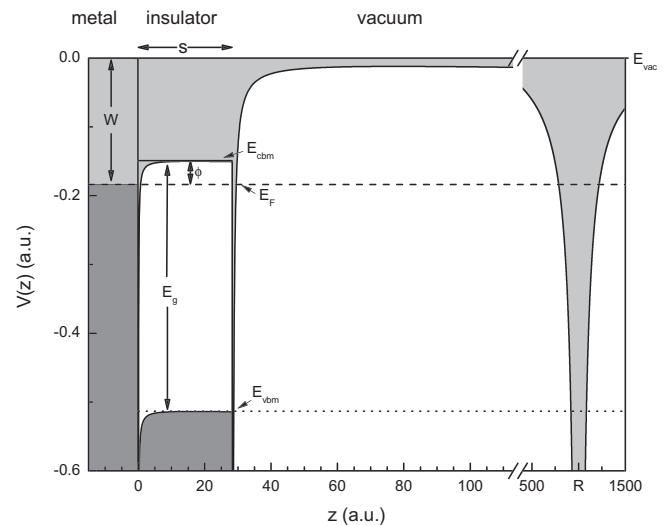


Fig. 2. The potential for an electron when an ion ($Q = 44$) is far away from a dielectric covered metal surface at $R = 1000$ a.u. The Fermi level in the metal is 5 eV (≈ 0.18 a.u.) below the vacuum level. The dielectric layer has thickness $s = 1.5$ nm (≈ 28 a.u.) with fixed band gap $E_g = 9.9$ eV (≈ 0.36 a.u.) and electrical permittivity $\epsilon = 9$. Electrons in the solid are restricted from entering the vacuum region by the barrier ϕ from $0 < z < s$ and the work function W outside s .

separating the ion and surface is diminished. The boundary condition that the potential from the ion and its image ($V_1 + V_{\text{int}}$) is set to zero at the surface of the metal is imposed.

3. Discussion

Using the framework presented above, we compare the potential for electrons originating from the metal and from the insulator to determine which path allows the first electron to travel classically to the ion. We determine the ion's distance from the metal R'_c where $V(0 < z < R) \leq E_F$ is met for electrons from the metal and $V(0 < z < R) \leq E_{\text{vbm}}$ is met for electrons from the insulator. We find that as the ion moves toward a surface with the parameters described above, transmission of electrons from the metal is allowed at much greater R than for the insulator.

Fig. 3(a) and (b) display $V(z)$ for ion positions $R = 250$ a.u. and $R = 118$ a.u. respectively. As the ion approaches the surface, two maxima in $V(z)$ exist, V_1 within the dielectric and V_2 within the vacuum (Fig. 3(a)). The ion's potential well (V_{int}) also bends the valence and conduction bands in the dielectric downward causing E_{cbm} and E_{vbm} to become more negative. In Fig. 3(a), V_2 has dropped far enough to equal E_F (dashed line). However, V_1 within the dielectric prevents over-barrier transmission from the metal. At $R = 250$ a.u., electrons in the insulator at E_{vbm} (dotted line), still face a thick tunnel barrier in the vacuum, i.e., $E_{\text{vbm}} \ll V_2$.

As the ion moves closer and approaches R'_c (Fig. 3(b)), V_1 drops and becomes equal to E_F . An electron in the metal can now transmit over both the barriers in the insulator (V_1) and vacuum (V_2) to the ion. The thick tunnel barrier for electrons at the top of the filled valence band of the film persists, $E_{\text{vbm}} \ll V_2$, preventing

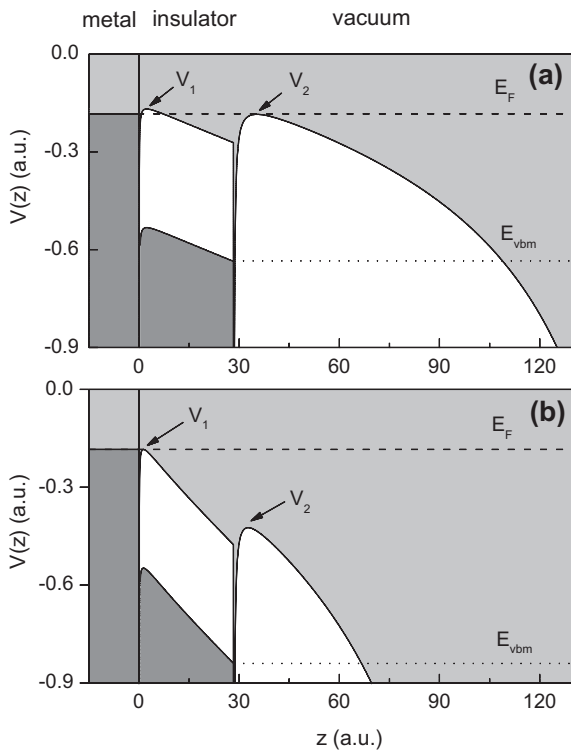


Fig. 3. Two $V(z)$ plots for a $Q = 44$ projectile above a dielectric covered metal surface at ion positions (a) $R = 250$ a.u. and (b) $R = 118$ a.u. E_F (dashed line) and E_{vbm} (dotted line) are the energies of electrons in the metal and insulator. Local maxima in the potential V_1 and V_2 that develop as the ion approaches the surface are shown in (a). Over-barrier transmission from the metal occurs when the height of these barriers falls below E_F . (b) depicts the critical distance R'_c for electrons from the metal from E_F (transmission from E_{vbm} in the insulator cannot proceed over-the-barrier).

over-barrier neutralization from the insulator. For quantitative comparison, at $R'_c(Q)$ the probability that an electron at E_{vbm} in the insulator can tunnel through the thick vacuum barrier is less than 10^{-22} for ions with charge states between $Q = 1$ and $Q = 44$. At R'_c electrons from E_F in the metal transmit classically to the ion with unity probability. Therefore, for the metal/insulator system described above, the first electron to participate in above-surface neutralization comes from the metal, not the exposed dielectric layer. $R'_c(Q)$ is shown in Fig. 4 for a range of charge states (filled squares). In the figure, the critical distances are adjusted to reflect the distance from the material-vacuum interface (the surface of the film) for purposes of comparing with CBM. A comparison between $R'_c(Q)$ and $R_c(Q, W = 5 \text{ eV})$ for the clean Co metal surface with $W = 5 \text{ eV}$ (short dashes) reveals that the dielectric film allows an electron to be captured at much larger distances. All charge states considered have R'_c values larger than R_c . For example, R'_c for a $Q = 44$ projectile above the insulator thin film/metal system is extended by 80% given parameters from Fig. 2. In the CBM expression $R_c(Q) = \sqrt{2Q}/W$ for a clean metal surface, the critical distance depends on the single energy barrier of height W . R'_c displays the same \sqrt{Q} dependence as $R_c(Q)$, but it was found that $R'_c(Q) \neq \sqrt{2Q}/W$ because using a constant W value for all Q does not fit the calculated R'_c values. Unlike R_c for a bulk target, over-barrier transmission of electrons from a metal covered with a dielectric film depends on two barriers ϕ and W (Fig. 2).

The $R'_c(Q)$ values do approach the single barrier case in the $Q \rightarrow 1$ and large Q limits. The $R_c(Q, W = 1 \text{ eV})$ plot shows the CBM predicted critical distances for $W = 1 \text{ eV}$. $R_c(Q, W = 1 \text{ eV})$ converges with R'_c at $Q = 1$. Solving $W = \sqrt{2Q}/R_c$ with $Q \rightarrow 85$ we find $W = 3.0 \text{ eV}$. The $R_c(Q, W = 3 \text{ eV})$ plot shows the CBM values for $W = 3 \text{ eV}$. $R'_c(Q)$ asymptotically approaches $R_c(Q, W = 3 \text{ eV})$ with increasing Q . This confirms that the CBM expression $R_c = \sqrt{2Q}/W$ does not predict critical distance for a target surface composed of two dielectric media even with a surrogate W . Rather, using CBM the effective barrier height for the metal/thin film system depends on Q and limits to 1 eV for $Q = 1$ and 3 eV for large Q in the case discussed.

As shown in Fig. 4, the dielectric film allows electrons to be captured at larger distances than for clean metal surfaces. Increased R_c

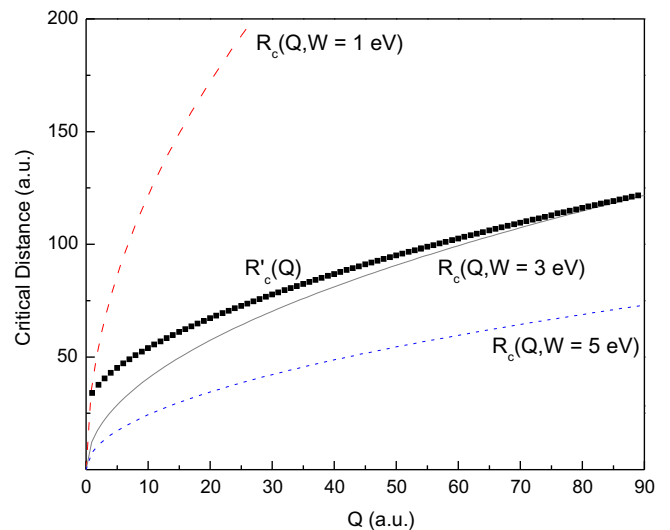


Fig. 4. (Color online). Critical distance for electron capture $R'_c(Q)$ with respect to the material-vacuum interface for HCl outside a Co surface with a 1.5 nm Al_2O_3 film (filled black squares) and CBM predictions based on $R_c(Q) = \sqrt{2Q}/W$, where $W = 1 \text{ eV}$ (long red dashes), $W = 3 \text{ eV}$ (solid gray line), and $W = 5 \text{ eV}$ (short blue dashes). The dielectric film extends the distance threshold for onset of above-surface neutralization compared to a clean metal with $W = 5 \text{ eV}$. Increased capture distances imply increased time for above-surface relaxation processes.

with the addition of the dielectric film can be explained through a reduction of the potential barrier height for electrons in the metal at position $z = 0$ and energy E_F . Instead of the barrier W that prevents electrons in a clean metal from entering the vacuum, the dielectric film lowers the energy barrier to height ϕ in the region $0 < z < s$. For the system shown in Figs. 2 and 4, the barrier within the dielectric is reduced with respect to the work function by the fraction $\phi/W = 0.2$. In this way, a thin dielectric layer lowers the potential barrier between the metal and vacuum. The film facilitates transmission from the metal to the vacuum over a lower barrier than the work function when the ion is in close proximity to the surface (Fig. 3(b)). For dielectric materials such as aluminum oxide, that have $E_{\text{cbm}} < E_{\text{vac}}$, ϕ is lower than W and a dielectric film will increase the critical distance. Based on this interpretation we expect that $R'_c < R_c$ for films with negative electron affinity such as LiF since $E_{\text{cbm}} > E_{\text{vac}}$ and the insulator would increase the potential barrier between the metal and vacuum.

Considering times after the first capture, the total above-surface electronic interaction time τ for an HCl is proportional to the distance for the onset of charge transfer ($\tau \sim R'_c(Q)$). Therefore, for the R_c and R'_c results shown in Fig. 4, the Al_2O_3 film increases τ by 80% for the $Q = 44$ charge state. Increased τ provides more time for inter- and intra-atomic Auger processes during above-surface neutralization and will likely increase the total electron emission yield compared to HCl interaction with a clean metal target.

Future modeling will test the dependence of $R'_c(Q)$ on the thickness s of the film as well as band gap and position of E_{cbm} with respect to the vacuum level. We expect that dielectric layers with negative electron affinity will inhibit electron transmission from the metal and decrease the ion's distance threshold for capture. Additionally, if s is increased significantly, the first electrons captured by the ion should eventually originate from the insulator instead of the metal.

4. Conclusion

We have presented a model based on the CBM for the beginning stages of above-surface HCl neutralization on a dielectric covered metal surface. The dielectric layer is described with the dielectric continuum model. Using parameters from a recent experiment with 1.5 nm thick Al_2O_3 insulating films on Co substrates, we found that the first electrons captured by the HCl come from the metal beneath the dielectric layer. Additionally it was shown that the film serves to extend the distance of first capture with respect to a clean metal system ($R'_c > R_c$). This effect is dependent on the positive electron affinity of the film and originates from the decreased energy barrier between E_F and E_{cbm} compared with the work function of a clean metal.

Acknowledgments

We gratefully acknowledge support from National Institute of Standards and Technology and the National Science Foundation.

References

- [1] H.P. Winter, F. Aumayr, J. Phys. B: At. Mol. Opt. Phys. 32 (1999) R39.
- [2] J. Burgdörfer, P. Lerner, F.W. Meyer, Phys. Rev. A 44 (1991) 5674.
- [3] L. Wirtz, C.O. Reinhold, C. Lemell, J. Burgdörfer, Phys. Rev. A 67 (2003) 012903.
- [4] J. Burgdörfer, Review of Fundamental Processes and Applications of Atoms and Ions, World Scientific, River Edge, NJ, 1993. Chap. 11, pp. 517–614.
- [5] R.E. Lake, J.M. Pomeroy, C.E. Sosolik, J. Phys.: Condens. Matter 22 (2010) 084008.
- [6] J. Güdde, W. Berthold, U. Hfer, Chem. Rev. 106 (2006) 4261.
- [7] W.M. Haynes (Ed.), CRC Handbook of Chemistry and Physics, 91st ed., (Internet Version 2011), CRC Press/Taylor and Francis, Boca Raton, FL.
- [8] J. M. Pomeroy, R. E. Lake, C. E. Sosolik, Nucl. Instrum. Meth. Phys. Res. Sect. B (2010), in press, doi:10.1016/j.nimb.2010.11.006.